

Document Version

Final published version

Licence

CC BY

Citation (APA)

Kenanoğlu, C. U., Wiertlewski, M., & Vardar, Y. (2026). Electrostatic Actuation Induces Competing Adhesion and Vibration Regimes at Fingertip Contact. *Advanced Intelligent Systems*, Article e70433. <https://doi.org/10.1002/aisy.70433>

Important note

To cite this publication, please use the final published version (if applicable). Please check the document version above.

Copyright

In case the licence states “Dutch Copyright Act (Article 25fa)”, this publication was made available Green Open Access via the TU Delft Institutional Repository pursuant to Dutch Copyright Act (Article 25fa, the Taverne amendment). This provision does not affect copyright ownership. Unless copyright is transferred by contract or statute, it remains with the copyright holder.

Sharing and reuse



Other than for strictly personal use, it is not permitted to download, forward or distribute the text or part of it, without the consent of the author(s) and/or copyright holder(s), unless the work is under an open content license such as Creative Commons.

Takedown policy

Please contact us and provide details if you believe this document breaches copyrights. We will remove access to the work immediately and investigate your claim.

RESEARCH ARTICLE OPEN ACCESS

Electrostatic Actuation Induces Competing Adhesion and Vibration Regimes at Fingertip Contact

Celal Umut Kenanoglu  | Michaël Wiertlewski  | Yasemin Vardar 

Department of Cognitive Robotics, Delft University of Technology, Delft, Netherlands

Correspondence: Yasemin Vardar (y.vardar@tudelft.nl)

Received: 30 January 2026 | **Revised:** 1 April 2026 | **Accepted:** 8 May 2026

Keywords: contact mechanics | electroadhesion | electrostatic actuation | electrovibration | haptics

ABSTRACT

Electrostatic actuation enables programmable tactile feedback by modulating finger-surface friction via oscillating electric fields. Despite its potential, widespread adoption is hindered by an incomplete understanding of the underlying physical mechanisms, particularly the dynamics of finger-surface contact. To address this problem, this study presents the first time-resolved measurements of real contact area modulation under electrostatic actuation, obtained concurrently with contact forces. Experiments with ten participants sliding their fingers on an electrostatic display revealed an inverted U-shaped dependence of mean contact area and tangential force on actuation frequency, with a pronounced peak near 116 Hz—consistent with the frequency-dependent response of the fingertip-display system captured by mass-spring-damper and contact models. Two regimes emerged: a vibration regime below 320 Hz, where the voltage increased the contact area more than the tangential force, thereby reducing interfacial shear stress relative to the baseline; and an adhesion regime at higher frequencies, where skin viscoelasticity attenuated oscillations and restored or increased shear stress. For moist fingers, vibration effects were reduced, weakening the modulation of both tangential force and contact area. These findings reveal how adhesion and vibration jointly govern finger-surface interactions, guiding the design of next-generation electrostatic haptic interfaces.

1 | Introduction

If you have ever run your fingertip along the metal edge of a laptop, the chassis of a smartphone, or the base of a desk lamp connected to AC power, you may have felt a subtle, almost sticky change in friction. This peculiar sensation is caused by *electrostatic actuation*, an electrically induced attractive force at the skin-surface interface. First documented a century ago by Johnsen and Rahbek as *electroadhesion* under a constant DC voltage [1], this phenomenon was shown to increase friction between human skin and charged surfaces. Decades later, Mallinckrodt et al. [2] applied an alternating voltage to insulated metal electrodes and discovered that the resulting electrostatic force caused the finger to be periodically attracted to and released from the surface—an effect now known as *electrovibration*. Electrostatic actuation has since become a widely used technology for producing tactile

feedback on surfaces, particularly on the touchscreens found in modern electronic devices [3].

Despite this long history, the mechanisms governing friction at the finger-surface interface under electrostatic actuation remain poorly understood. The increase in frictional force observed under such electrical loading is commonly attributed to an increase in real contact area, consistent with the adhesion model proposed by Bowden and Tabor [4]. In this model, the kinetic friction is expressed as $F_t = \tau A$, where A is the real contact area formed by microscopic asperity junctions, and τ denotes the interfacial shear stress during sliding [5]. Prior studies have primarily interpreted the rise in friction by assuming that electrostatic loading increases A , while leaving τ constant [6–8], often relying on multiscale mean-field contact theory [9, 10] to infer area changes from measured tangential forces.

This is an open access article under the terms of the [Creative Commons Attribution](https://creativecommons.org/licenses/by/4.0/) License, which permits use, distribution and reproduction in any medium, provided the original work is properly cited.

© 2026 The Author(s). *Advanced Intelligent Systems* published by Wiley-VCH GmbH.

In haptic displays, however, electrostatic actuation is typically applied as an oscillating voltage at frequencies ranging from tens to hundreds of hertz to provide tactile feedback. The resulting electrostatic force therefore oscillates in time, periodically loading and unloading the fingertip and imposing a vibration on the contact. Although the magnitude of this motion—its effect on the finger contact area and resulting friction—inevitably depends on fingertip mechanics, most prior studies have primarily interpreted frequency-dependent friction changes from an electrical perspective, attributing them to variations in the impedance of the finger-screen interface [8, 11–13]. While this view explains how electrostatic pressure varies with frequency, it does not address how a fingertip responds to time-varying loading or how this loading alters instantaneous contact behavior during sliding. Recent measurements reveal a high-frequency attenuation in friction even when the electrical behavior is held approximately constant, consistent with a first-order, low-pass mechanical response of the fingertip [14]. This attenuation points to a direct vibrational contribution to friction, in line with findings on fingertip contact under pure mechanical loading. For example, ultrasonic oscillations reduce sliding finger friction [15, 16]. Moreover, dynamic loading reduces the tangential force more than the contact area with increasing frequency, thus varying interfacial shear stress [17]. Collectively, these findings indicate that vibration reshapes fingertip contact mechanics during sliding by attenuating friction that counteracts adhesion.

Taken together, these studies show that adhesion and vibration exert opposing effects on friction. Under oscillating electrostatic actuation on haptic touchscreens, these mechanisms operate simultaneously: the electric field generates an average attractive normal load that increases friction (adhesion), while its temporal modulation repeatedly pulls and releases the fingertip, imposing an oscillating motion on the contact (vibration). Their coexistence has led to a nearly interchangeable use of terms (*electro*) *adhesion*, referring to electrically induced attraction of the skin toward the surface, and (*electro*) *vibration*, referring to oscillatory

fingertip motion perceived by the user, even though they describe distinct physical phenomena. What remains unknown is how these antagonistic contributions, in combination with the fingertip's mechanical response to the oscillating field, jointly determine the frequency dependence of contact area, tangential force, and interfacial shear stress under electrostatic actuation. Establishing this missing link is essential for explaining the mechanisms governing friction at the finger-surface interface and for designing haptic interfaces that control friction reliably through electrostatic fields.

Here, we show how these two fundamentally opposing phenomena, adhesion and vibration, jointly shape finger-surface contact under an oscillating electric field by combining, for the first time, time-resolved friction measurements with synchronized imaging of contact area. The results indicate the existence of two distinct regimes, *vibration* and *adhesion*, with respect to frequency (Figure 1). In the vibration regime, oscillatory motion enhances the contact area more than the tangential force, lowering interfacial shear stress (area-normalized tangential force) relative to the voltage-off reference. At higher frequencies, however, the increase in tangential force dominates, raising interfacial shear stress and marking a transition to an adhesion-dominated regime. This shift reflects the fingertip's viscoelastic inability to follow rapid oscillations, a mechanism captured by a spring-damper model of the fingertip coupled with contact and friction models. Finally, all measured quantities exhibit substantial interparticipant variability, reflecting differences in fingertip mechanics and skin moisture.

2 | Results

We measured fingertip–touchscreen interaction in 10 participants under controlled conditions of normal force and speed, both with and without electrostatic actuation. Data were collected at 10 logarithmically spaced frequencies (25–2500 Hz), with three repetitions per condition. An overview of the experimental setup and

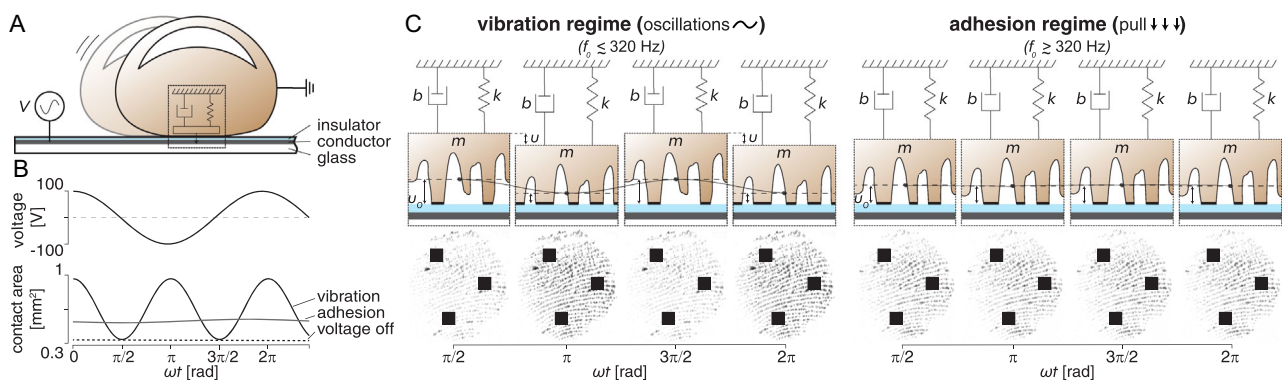


FIGURE 1 | Frequency-dependent contact behavior under electrostatic actuation: vibration and adhesion regimes. (A) Schematic of a sliding fingertip on an electrostatic touchscreen, modeled as a lumped spring-mass-damper system. (B) Sinusoidal drive voltage and phase-dependent modulation of real contact area in two regimes; the dashed line indicates the 0-V baseline. (C) Response of the fingertip model in the normal direction, where k , m , and b represent spring, effective mass, and damping coefficients. Insets illustrate the micro-junction behavior in the two regimes: dynamic, oscillatory contact in the vibration regime and sustained, pulled-in contact in adhesion regime. The sinusoidal drive voltage $V(t) = V_0 \cos(\omega t)$, where $\omega = 2\pi f_0$ is the angular frequency corresponding to the input frequency f_0 and t is time, is shown at its extrema and at a zero crossing. The dashed line in the insets marks the nominal interfacial separation, u_0 . At low frequencies ($f_0 \lesssim 320$ Hz), vibration induces oscillatory skin motion, leading to phase-dependent modulation of real contact area. At higher frequencies, adhesion dominates, pulling the skin toward the surface and increasing contact area relative to the voltage-off reference.

protocol, along with the recorded signals, is shown in Figure 2; more details are provided in Materials and Methods and Figures S1–S4.

Electrostatic actuation induced oscillations in both tangential force and real contact area at twice the input frequency f_0 , consistent with the quadratic dependence of electrostatic force on voltage [13, 18] (Figures 2C and S5). Both signals reached maxima near the voltage peak extrema (± 100 V) and minima at the zero-crossings ($V = 0$), where their values matched those measured under the voltage-off condition (Figures 2C and 3A).

Temporal modulation of real contact area over the drive cycle was clearly visible in the FTIR images, where darker regions correspond to greater contact (Figure 3A; Movies S1 & S2).

Changes in tangential force and real contact area across frequencies were quantified as the ratio of voltage-on to voltage-off values (i.e., with and without electrostatic actuation), computed within the same trial to ensure consistency. Throughout the manuscript, metrics averaged over the interval during which electrostatic actuation was applied are denoted by the superscript “on”, whereas those obtained without actuation are denoted by

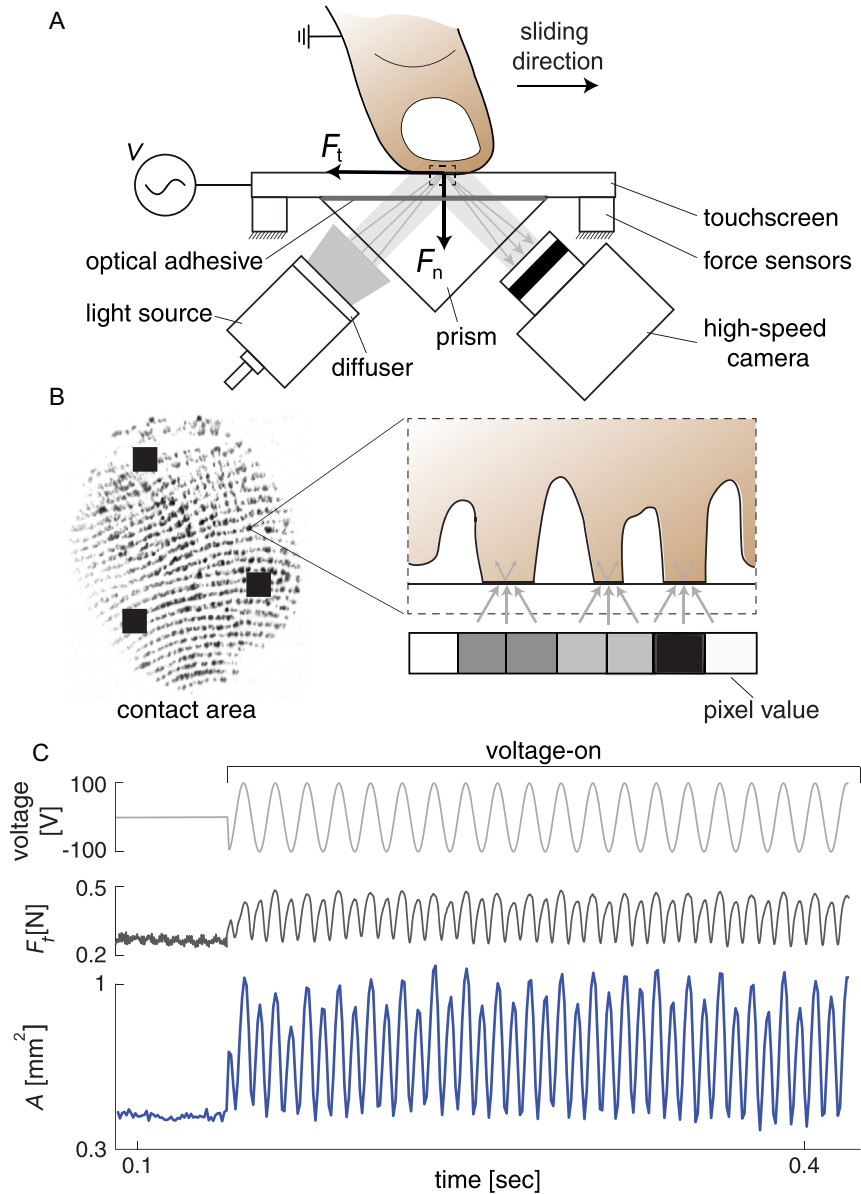


FIGURE 2 | Experimental setup and representative measurements. (A) Schematic of the setup for simultaneous measurement of contact area and tangential force (F_t) during finger sliding on a touchscreen under electrostatic actuation. A prism-based frustrated total internal reflection (FTIR) system illuminates the contact zone from below, allowing for direct imaging of fingertip contact using a high-speed camera and diffused light source. The touchscreen is optically bonded to the prism. Participants slid their finger at a constant normal force ($F_n = 1$ N) and speed (20 mm/s). During the initial one-third of each trial, the touchscreen was inactive (voltage-off), behaving as smooth glass, after which an alternating voltage (100 V peak) was applied to activate electrostatic actuation. Tangential force (F_t), normal force (F_n), fingertip contact area (A), and current were recorded throughout. (B) Principle of contact imaging with an example FTIR image. Light is totally internally reflected within the prism except at microscopic ridge asperities in intimate contact, where scattering causes dark pixels; noncontact regions remain bright. (C) Representative trial data showing input voltage, tangential force, and real contact area over time.

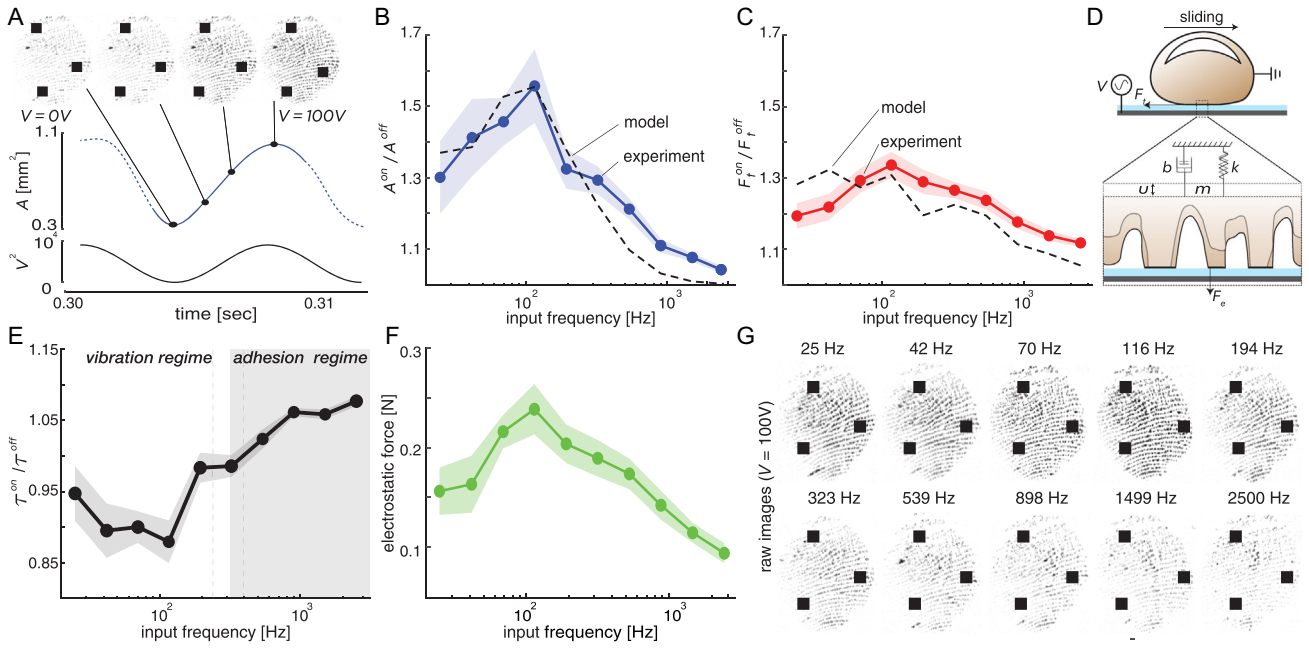


FIGURE 3 | Experimental results. (A) Time evolution of the contact area at 70 Hz, illustrating oscillations induced by electrostatic actuation. (B,C) Ratio of measured contact areas (A^{on}/A^{off}) and tangential forces (F_t^{on}/F_t^{off}) with and without electrostatic actuation across frequencies and corresponding model predictions [9, 10, 15, 19, 20]. (D) Lumped spring-mass-damper model of the fingertip dynamics, where an electrostatic force F_e induces normal displacement u that increases the number of micro-junctions, thereby increasing the real contact area and tangential force, F_t . (E) Interfacial shear stress ratio $\tau^{on}/\tau^{off} = (F_t^{on}A^{off})/(F_t^{off}A^{on})$. The transition zone around 320 ± 82 Hz (between dashed lines) separates the vibration regime ($\tau^{on}/\tau^{off} < 1$) from the adhesion regime ($\tau^{on}/\tau^{off} \geq 1$). (F) Estimated electrostatic force $(1 - \mu_{off}/\mu_{on})F_n$ [8, 21, 22]. (G) Representative FTIR images of fingertip contact at different frequencies (100 V). Darker regions indicate greater contact, with stronger modulation in the vibration regime than in the adhesion regime. In B–F, large circles denote participant means, shaded bands indicate standard error of the mean, and superscripts “on/off” denote voltage on/off.

“off”. For both measures, these ratios exceeded unity at all tested frequencies, confirming the effect of electrostatic actuation (Figures 3B,C and S6–S8). Moreover, they increased with frequency up to approximately 116 Hz, after which they declined. Below 320 ± 82 Hz, the relative increase in contact area exceeded that of tangential force across participants, whereas above this frequency the trend reversed, with tangential force showing a slightly greater increase.

The measured real contact areas and tangential forces were compared with predictions from a spring-mass-damper model [15], a mean-field contact model based on Persson’s contact theory [9, 10, 15], and a quasi-static model [19] to investigate whether these existing frameworks are consistent with the observed frequency-dependent behavior. The spring-mass-damper model was used to illustrate the fingertip’s mechanical response to electrostatic actuation in the normal direction, with the electrostatic force estimated as $F_e = (1 - \mu_{off}/\mu_{on})F_n$, where μ is the measured friction coefficient and F_n is the applied normal load. The resulting vertical displacement, u , was then used as input to the mean-field and quasi-static models to estimate, respectively, the modulation of real contact area and tangential force. Then, the estimated contact area and tangential force ratios from the models were compared with the ones obtained from experimental measurements (Figure 3B–D). In the mean-field contact model, the contact area depends on the microscale surface roughness and the applied normal pressure. The displacement u modulated the contact area as $A^{on} = A^{off} \exp(u_m/u_{rms})$, where u_{rms} is the

microscale root-mean-square roughness of the fingertip surface, and u_m is the microscale displacement, obtained by scaling u with a dimensionless macro-to-micro factor. The resulting contact area exhibited a peak near 116 Hz and decreased at higher frequencies (Figures 3B and S9–S11). The model output showed good agreement with the experimentally measured contact-area trend across frequencies, with relative errors ranging from 0.16% to 9.45% and a mean absolute error of 4.7% (Figure 3B). The macroscale quasi-static model [19], which incorporates contact stiffness in normal and tangential directions, was used to examine the influence of normal vibration on tangential force. This model provides a physically interpretable approximation of the reduced increase in tangential force under oscillatory loading. Using the displacement estimated by the spring-mass-damper model, u , as input, the predicted tangential force trend closely matched the experimental trends, with errors ranging from 1.5% to 8.5% and a mean absolute error of 4.9% (Figures 3C and S12–S13). However, the quasi-static model does not explicitly account for frequency-dependent viscoelastic and electrical effects; therefore, its validity is limited at higher frequencies, where these mechanisms become increasingly important. Further details of the model implementation are provided in the Supplementary Materials.

To assess the effects of frequency and participant variability, a linear mixed-effects model was employed for the A^{on}/A^{off} and F_t^{on}/F_t^{off} ratios. Frequency was modeled as a fixed effect, and participant identity as a random intercept. The models revealed

significant effects of frequency on both real contact area ($F(9,90) = 12.43$, $p < 0.001$) and tangential force ($F(9,90) = 10.37$, $p < 0.001$). Likelihood ratio tests comparing full models (with random effects) to reduced models (without) confirmed substantial interparticipant variability for both measures: real contact area ($\chi^2(1) = 30.94$, $p < 0.001$) and tangential force ($\chi^2(1) = 23.43$, $p < 0.001$).

The pronounced frequency-dependent changes in real contact area and tangential force under electrostatic actuation indicated that interfacial shear stress was not constant, contradicting assumptions made in previous studies [6–8]. The interfacial shear stress ratio, τ^{on}/τ^{off} , calculated using the relation $F_t = \tau A$, exhibited clear frequency-dependent variations (Figures 3E and S14). Below 320 ± 82 Hz, the increase in tangential force was less than the corresponding increase in contact area ($F_t^{on}/F_t^{off} < A^{on}/A^{off}$), yielding $\tau^{on}/\tau^{off} < 1$ and defining the *vibration* regime. This transition frequency represents the average across participants, with individual variability indicated by the light-gray shaded region in Figure 3E. Above this frequency, $\tau^{on}/\tau^{off} \geq 1$, marking the onset of the *adhesion* regime. See Figures S15–S18 for tangential force and contact area measurements from both regimes.

A linear mixed-effects model confirmed that the interfacial shear stress ratio (τ^{on}/τ^{off}) varied significantly with frequency ($F(9,90) = 19.49$, $p < 0.001$). Post hoc paired t-tests with Benjamini–Hochberg correction revealed significant differences in τ^{on}/τ^{off} between frequencies across the vibration and adhesion regimes

($p < 0.05$), with the strongest contrast observed between the 70–116 Hz range and the adhesion regime ($p < 0.001$). A likelihood-ratio test comparing a model including participant identity as a random effect to one without indicated a superior fit for the full model ($\chi^2(1) = 33.32$, $p < 0.001$), confirming interparticipant variability. See Figures S19–S21 for detailed pairwise results.

The electrostatic force also showed a frequency-dependent trend, rising to a peak near 116 Hz and then declining at higher frequencies (Figure 3F). A linear mixed-effects model revealed a significant effect of frequency ($F(9,90) = 12.19$, $p < 0.001$). A likelihood-ratio test comparing models with and without participant identity as a random effect confirmed significant interparticipant variability ($\chi^2(1) = 44.99$, $p < 0.001$). The shaded region in Figure 3F illustrates this variability, which was more pronounced in the vibration regime.

Fingerprint images also revealed pronounced frequency-dependent variations in real contact area (see Figure 3G for representative data from one participant). The intensity of the black regions, corresponding to skin asperities at contact, was consistently greater at 100 V than at 0 V across all frequencies (see also Figure 3A). The real contact area was larger in the vibration regime than in the adhesion regime, consistent with the stronger influence of the electrostatic force at lower frequencies. To examine spatial patterns, we visualized fingerprint contact distributions with colormaps (Figure S22), which show that electrostatic actuation primarily enhances central contact, which is already evident in the raw

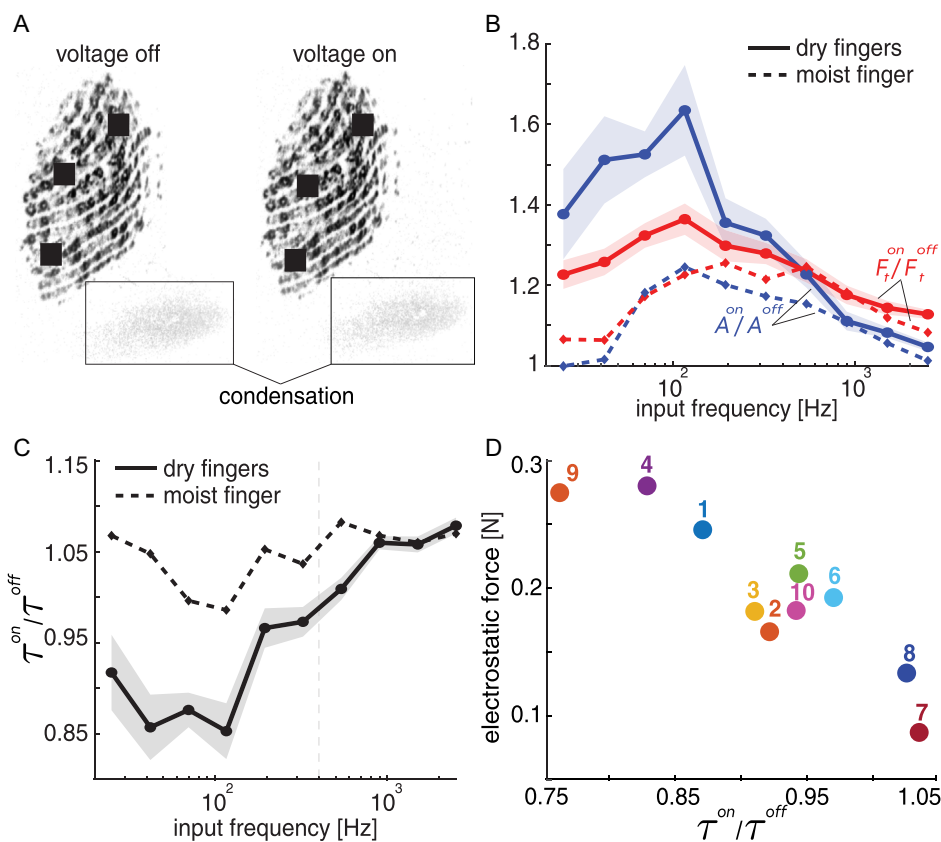


FIGURE 4 | Effect of moisture on electrostatic actuation. (A) Representative fingerprint images showing condensation, indicating the presence of moisture. (B) Ratios of voltage on/off ratios values for real contact area and tangential force. (C) Interfacial shear stress comparing participants with moist and dry fingers. (D) Mean electrostatic force within the vibration regime for each participant.

images (Figure 3A,G). A qualitative comparison of the central and peripheral contact regions further indicated that the central enhancement was more pronounced in the vibration regime (Figure S23). Consistent with this observation, a 1D relative gap analysis along the middle of the fingerprint image showed that the difference between 100 and 0 V remained relatively small near the contact edges but became more pronounced toward the center (Figure S24). Representative videos of the fingertip contact during the vibration and adhesion regimes are provided in Movies S1–S4.

Lastly, we observed condensation in the fingerprint images of some participants (Figure 4A and Movie S5), indicating the presence of finger moisture, as observed in previous studies [23–26]. For these participants, both the changes in real contact area and tangential force between the voltage-on and voltage-off conditions were smaller (Figure 4B). Correspondingly, the reduction in interfacial shear stress under electrostatic actuation was less pronounced compared to participants with drier fingers, whose images did not exhibit condensation (Figure 4C). Within the vibration regime, participants with moist fingers exhibited a mean interfacial shear stress ratio that was 15.3% higher than those with dry fingers. When moist-finger data were excluded, the transition frequency shifted upward to 400 Hz. During this regime, participants with moist fingers showed lower electrostatic force and electrical impedance (Figures 4D, S25–S27). Across participants, larger reductions in interfacial shear stress under voltage-on conditions were associated with higher electrostatic force, with a similar but weaker trend for electrical impedance (Figure 4D).

3 | Discussion

Fingertip contact on electrostatic displays is shaped by oscillating electric fields that attract the fingertip toward the surface, thereby modifying the real contact area and friction at the skin-glass interface. By directly measuring time-resolved contact area and forces, we demonstrate that the frequency of electrostatic actuation governs fingertip-surface interactions, giving rise to two regimes: a *vibration* regime at low frequencies and an *adhesion* regime at high frequencies. These regimes produce characteristic changes in tangential force, real contact area, and interfacial shear stress. In the vibration regime, the increase in contact area exceeds the rise in tangential force between voltage-on and voltage-off conditions, resulting in a net reduction in interfacial shear stress. While electrostatic adhesion increases both friction and contact area regardless of frequency, at low frequencies, vibration weakens the adhesive contribution to tangential force, thereby reducing overall frictional enhancement. This vibration-induced friction reduction is consistent with prior observations across a range of materials and systems [15, 17, 19, 27, 28]. In this regime, electrostatic actuation induces periodic normal force oscillations that diminish the effective mechanical coupling between the fingertip and the touchscreen, leading to a decrease in interfacial shear stress [17]. According to the quasi-static model [19], these oscillations promote stick-slip dynamics at the interface, producing intermittent slipping and a reduction in effective tangential force—consistent with the displacement predicted by the spring-mass-damper model (Figure S9). A similar reduction in the interfacial shear stress has been reported for

finger-glass interaction under mechanical vibration [17], supporting the interpretation that vibration primarily reduces tangential force rather than contact area. Analysis of supplementary videos (Movies S1 & S2) further revealed clear within-cycle modulation of tangential motion at low frequencies, including pronounced ($2f_0$) components in instantaneous velocity (Figure S28). This behavior is consistent with partial stick-slip motion, supported by corresponding within-cycle modulation in instantaneous interfacial shear stress (Figure S29).

Notably, the observed peak around 116 Hz in contact area, tangential force, and interfacial shear stress ratio coincides with both the frequencies of enhanced tactile sensitivity of electrovibration [13] and the normal-direction resonant modes of the fingertip [29]. This agreement suggests that the pronounced low-frequency vibratory effects arise from the combined influence of the electrical properties of the finger-display system and fingertip mechanics (Figure S30).

At frequencies above 320 ± 82 Hz, the interfacial shear stress ratio between the voltage-on and voltage-off conditions exceeds unity, marking the transition to the adhesion regime. In this regime, the fingertip is less able to mechanically track rapid oscillations due to the constraints imposed by its intrinsic viscoelastic response [14, 30]. Consistently, previous studies modeling finger-touchscreen interaction under electrostatic actuation as a spring-mass-damper system have also shown that the system behaves as a low-pass filter, with induced oscillations attenuating above 300 Hz [14]. This behavior aligns with the interval-averaged differences observed here between the vibration- and adhesion-dominated regimes. As the vibration component of electrostatic actuation diminishes, adhesive effects become dominant, yielding interfacial shear stress above baseline ($\tau^{\text{on}}/\tau^{\text{off}} \geq 1$). Crucially, this adhesion-dominated regime does not reflect increased intrinsic adhesive strength; rather, it results from the skin's limited ability to track high-frequency oscillations, reinforcing a continuous contact state. This physical transition aligns with qualitative feedback from participants, who described a distinct “stickier” sensation in the adhesion regime compared to the “vibratory” feel at lower frequencies.

Furthermore, the inverted U-shaped frequency response observed in electrostatic force, real contact area, and tangential force arises from the coupled mechanical and electrostatic dynamics at the interface. The vertical electrostatic attraction between the finger and surface increases the real contact area, which in turn enhances tangential force. A similar U-shaped trend in electrostatic force was reported in [8, 22], where the decrease at low frequencies was attributed to charge drift toward the outer surface of the stratum corneum [6–8]. At high frequencies, the frequency-dependent dielectric properties of the stratum corneum limit sufficient charge migration within each oscillation cycle ($T = 2\pi/\omega$), thereby reducing the effectiveness of electrostatic actuation. This interpretation is supported by electrical impedance measurements of the finger-touchscreen [18, 22, 31, 32], which similarly showed a reduction at higher frequencies, consistent with reduced electrostatic force.

Across participants, the modulation of contact area, tangential force, and interfacial shear stress varied significantly, reflecting individual differences in skin moisture and electrical properties.

Participants with moist fingers exhibited lower electrostatic force and electrical impedance, consistent with prior findings that skin hydration enhances conductivity and reduces the effective air gap, weakening the electric field at the interface [32]. Although these individuals showed greater baseline friction and contact area without actuation [24, 26, 32, 33], they exhibited much smaller relative increases with electrostatic loading. This behavior can be attributed to greater effective damping in moist skin, which limits vertical displacement and reduces the modulation of tangential force and contact area. These findings indicate that increased skin moisture primarily suppresses the vibratory component of electrostatic actuation.

Beyond moisture, additional interparticipant differences in fingerpad curvature and skin mechanics likely contributed to observed variability. As shown in Figures 3G and S22–S24, electrostatic actuation tended to increase contact area near the fingertip center, where vertical electrostatic force draws the skin toward the surface. The magnitude and spatial distribution of this expansion varied across participants. The transition frequency separating the vibration and adhesion regimes also differed across participants, further reflecting mechanical and geometric variability. Together, these electrical, mechanical, and physiological differences constrain the uniformity of electrostatic modulation of fingertip-surface interactions.

Despite careful investigation, this study has several limitations. First, the FTIR-based imaging and analysis method [34] provides an optically resolved measure of fingertip-glass real contact area and may not capture its absolute magnitude at the nanoscale. As real contact area is inherently scale-dependent, multiscale approaches combining optical and AFM measurements suggest that unresolved sub-optical roughness can influence its absolute value [35]. Accordingly, this limitation may affect the absolute magnitude of the measured area; nonetheless, the present study focuses on relative changes measured consistently across conditions. Second, the dynamic bandwidth of the experimental setup may attenuate high-frequency oscillations. Consequently, the analysis primarily relies on interval-averaged metrics rather than fully resolved instantaneous oscillation amplitudes (see Supplementary Material and Figure S31 for details). Finally, the interparticipant differences were inferred from image condensation, electrical impedance, and electrostatic force; direct measurements of skin hydration and other biomechanical properties were not performed. Incorporating such measurements in future work would provide a stronger foundation for interpreting interparticipant variability in electrostatic actuation.

From a haptic display design perspective, the present results identify distinct operating regimes for electrostatic interfaces under conditions comparable to those studied here. Frequencies in the vibration-dominated regime, particularly near the observed peak around 116 Hz, are well suited for enhancing dynamic contact modulation and vibratory tactile feedback. In contrast, frequencies above the transition near 320 Hz, where oscillatory skin deformation is attenuated and interfacial shear stress is restored or increased, are more appropriate for interactions intended to feel more adhesive or drag-like. The reduced modulation observed for moist fingers further indicates that practical devices may benefit from adaptive or user-dependent tuning rather than fixed actuation parameters.

In conclusion, our direct measurements of finger contact-area modulation under oscillating electric fields demonstrate that contact dynamics of sliding fingers on electrostatic displays are jointly governed by the interplay of vibration and adhesion, with vibratory effects diminishing at higher frequencies due to the electromechanical response of the finger-display system. These findings provide a mechanistic foundation for electrostatic haptic interfaces and support the development of more reliable, adaptive, and skin-condition-aware designs.

4 | Materials and Methods

The experiment was conducted with ten participants (seven men, three women; mean age: 27, SD: ± 2.45). The study was conducted by adhering the Declaration of Helsinki and approved by the Ethics Council of TU Delft (application no. 5108). All participants provided informed consent.

The participants slid their right-hand index finger across a capacitive touchscreen (SCT3250, 3 M Inc.), which was electrostatically actuated by an alternating voltage applied to its conductive layer. The voltage signal was generated using a data acquisition card (PCIe 6321, NI Inc.) and amplified by a high-voltage amplifier (9200A, Tabor Electronics). Participants wore an antistatic wrist strap during the experiment. The touchscreen was mounted on two six-axis force sensors (Nano17 Titanium, ATI Inc.) to record contact forces at a sampling rate of 10 kHz. Finger motion was controlled by a motorized linear stage (NRT150/M, Thorlabs Inc.) set at a fixed contact angle of 60°. Electrical impedance was measured via a differential probe and shunt resistor positioned between the amplifier and the touchscreen. Fingertip contact area was recorded using a high-speed camera at 1000 fps (MotionBLITZ EoSens mini2, Mikrotron) with a lens (LM16HC, Kowa) mounted beneath the glass, employing the FTIR method [17]. The glass was illuminated using a light source (KL 2500 LED, Schott) fitted with a custom collimation package and diffuser. The touchscreen assembly was mounted on damped posts attached to an optical breadboard to minimize transmission of external vibrations. Data acquisition from the force sensors, linear stage control, and camera triggering were synchronized using MATLAB Simulink. Force and impedance data were collected through Simulink, while contact images were captured using MotionBLITZ software. Real contact area was computed from contact images following [34]. See Supplementary Material for details of data extraction and analysis.

Before the experiment, participants were instructed to wash their hands and wipe them with a microfiber cloth. During each trial, the participant's finger was moved laterally at a constant speed of 20 mm/s while maintaining a normal force of 1 N, guided by real-time LED feedback. Data were recorded only when the applied normal force was within $\pm 10\%$ of the target, and the fingerprint image was clearly visible. Electrostatic actuation was applied during the same sliding motion using alternating conditions: voltage-off and voltage-on at 100 V. Ten logarithmically spaced sine wave frequencies (25–2500 Hz) were tested, each with three repetitions. The full experimental session lasted approximately 30 min per participant. To minimize variability due to moisture, participants wiped their fingertips with a microfiber cloth before

each trial, and a fan was used to maintain consistent skin dryness.

Author Contributions

Celal Umut Kenanoglu: conceptualization, methodology, investigation, software, hardware, formal analysis, data curation, visualization, writing – original draft. **Michaël Wiertlewski:** conceptualization, methodology, formal analysis, visualization, writing – review & editing, supervision. **Yasemin Vardar:** conceptualization, methodology, formal analysis, visualization, writing – original draft, writing – review & editing, supervision, resources, project administration, funding acquisition.

Declaration of Generative AI and AI-Assisted Technologies in the Writing Process

The authors used OpenAI's ChatGPT and Grammarly Inc.'s Grammarly for language editing and readability improvements; the authors are responsible for all content and the final manuscript.

Funding

This work has been partially supported by the Dutch Research Council, NWO (Grant 19153 and 20624) (YV) and the Innovation in Haptics grant from the Technical Committee on Haptics (CUK).

Conflicts of Interest

The authors declare no conflicts of interest.

Data Availability Statement

The dataset used in this study is publicly available via 4TU. ResearchData under the following <http://doi:10.4121/73fcb6-be65-4e04-a818-aa04601dbaf4>.

References

1. A. Johnsen and K. Rahbek, "A Physical Phenomenon and Its Applications to Telegraphy, Telephony, etc.," *Journal of the Institution of Electrical Engineers* 61, no. 320 (1923): 713–725.
2. E. Mallinckrodt, A. Hughes, and W. Sleator Jr, "Perception by the Skin of Electrically Induced Vibrations," *Science* 118, no. 3062 (1953): 277–278.
3. O. Bau, I. Poupyrev, A. Israr, and C. Harrison, "TeslaTouch: electrovibration for touch surfaces," in Proceedings of the 23rd Annual ACM Symposium on User Interface Software and Technology (UIST '10), (Association for Computing Machinery, 2010), 283–292.
4. F. P. Bowden and D. Tabor, *The Friction and Lubrication of Solids* (Oxford University Press, 2001).
5. X. He, Z. Liu, L. B. Ripley, et al., "Empirical Relationship between Interfacial Shear Stress and Contact Pressure in Micro- and Macro-Scale Friction," *Tribology International* 155 (2021): 106780.
6. M. Ayyildiz, M. Scaraggi, O. Sirin, C. Basdogan, and B. N. Persson, "Contact Mechanics between the Human Finger and a Touchscreen under Electroadhesion," *Proceedings of the National Academy of Sciences* 115, no. 50 (2018): 12668–12673.
7. O. Sirin, M. Ayyildiz, B. N. Persson, and C. Basdogan, "Electroadhesion with Application to Touchscreens," *Soft Matter* 15, no. 8 (2019): 1758–1775.
8. E. AliAbbasi, M. A. Sormoli, and C. Basdogan, "Frequency-Dependent Behavior of Electrostatic Forces between Human Finger and Touch Screen under Electroadhesion," *IEEE Transactions on Haptics* 15, no. 2 (2022): 416–428.
9. B. N. Persson, "Contact Mechanics for Randomly rough Surfaces," *Surface Science Reports* 61, no. 4 (2006): 201–227.

10. B. N. J. Persson, "The Dependency of Adhesion and Friction on Electrostatic Attraction," *The Journal of Chemical Physics* 148, no. 14 (2018): 144701.
11. C. D. Shultz, M. A. Peshkin, and J. E. Colgate, "Surface Haptics via Electroadhesion: Expanding Electro-vibration with Johnsen and Rahbek," In Proceedings of the 2015 IEEE World Haptics Conference (WHC), (IEEE, 2015): 57–62.
12. B. N. Persson, "General Theory of Electroadhesion," *Journal of Physics: Condensed Matter* 33, no. 43 (2021): 435001.
13. Y. Vardar, B. Güçlü, and C. Basdogan, "Effect of Waveform on Tactile Perception by Electro-vibration Displayed on Touch Screens," *IEEE Transactions on Haptics* 10, no. 4 (2017): 488–499.
14. J. K. Balasubramanian, D. M. Pool, and Y. Vardar, "Sliding Speed Influences Electro-vibration-Induced Finger Friction Dynamics on Touchscreens," *Tribology International* 213, no. 11105 (2026): 2026.
15. M. Wiertlewski, R. Fenton Friesen, and J. E. Colgate, "Partial Squeeze Film Levitation Modulates Fingertip Friction," *Proceedings of the National Academy of Sciences* 113, no. 33 (2016): 9210–9215.
16. E. Vezzoli, Z. Vidrih, V. Giamundo, et al., "Friction Reduction through Ultrasonic Vibration Part 1: Modelling Intermittent Contact," *IEEE Transactions on Haptics* 10, no. 2 (2017): 196–207.
17. S. Bochereau, B. Dzidek, M. Adams, and V. Hayward, "Characterizing and Imaging Gross and Real Finger Contacts under Dynamic Loading," *IEEE Transactions on Haptics* 10, no. 4 (2017): 456–465.
18. Y. Vardar and K. J. Kuchenbecker, "Finger Motion and Contact by a Second Finger Influence the Tactile Perception of Electro-vibration," *Journal of the Royal Society Interface* 18, no. 176 (2021): 20200783.
19. M. Popov, "The Influence of Vibration on Friction: A Contact-Mechanical Perspective," *Frontiers in Mechanical Engineering* 6 (2020): 69.
20. B. Persson, A. Kovalev, and S. Gorb, "Contact Mechanics and Friction on Dry and Wet Human Skin," *Tribology Letters* 50 (2013): 17–30.
21. C. Basdogan, M. R. A. Sormoli, and O. Sirin, "Modeling Sliding Friction between Human Finger and Touchscreen under Electroadhesion," *IEEE Transactions on Haptics* 13, no. 3 (2020): 511–521.
22. E. AliAbbasi, Ø.G. Martinsen, F.-J. Pettersen, J. E. Colgate, and C. Basdogan, "Experimental Estimation of Gap Thickness and Electrostatic Forces between Contacting Surfaces under Electroadhesion," *Advanced Intelligent Systems* 6, no. 4 (2024): 2300618.
23. S.-M. Yum, I.-K. Baek, D. Hong, et al., "Fingerprint Ridges Allow Primates to Regulate Grip," *Proceedings of the National Academy of Sciences* 117, no. 50 (2020): 31665–31673.
24. G. Serhat, Y. Vardar, and K. J. Kuchenbecker, "Contact Evolution of Dry and Hydrated Fingertips at Initial Touch," *PLoS One* 17, no. 7 (2022): e0269722.
25. R. E. Boseley, J. Vongsvivut, D. Appadoo, M. J. Hackett, and S. W. Lewis, "Monitoring the Chemical Changes in Fingerprint Residue over Time Using Synchrotron Infrared Spectroscopy," *The Analyst* 147, no. 5 (2022): 799–810.
26. V. H. P. Infante, M. Fehlberg, S. Saikumar, K. DREWING, M. C. Meinke, and R. Bennewitz, "The Role of Skin Hydration, Skin Deformability, and Age in Tactile Friction and Perception of Materials," *Scientific Reports* 15, no. 1 (2025): 9935.
27. H. D. Fridman and P. Levesque, "Reduction of Static Friction by Sonic Vibrations," *Journal of Applied Physics* 30, no. 10 (1959): 1572–1575.
28. V. L. Popov, J. Starcevic, and A. E. Filippov, "Influence of Ultrasonic in-Plane Oscillations on Static and Sliding Friction and Intrinsic Length Scale of Dry Friction Processes," *Tribology Letters* 39 (2010): 25–30.
29. G. Serhat and K. J. Kuchenbecker, "Fingertip Dynamic Response Simulated across Excitation Points and Frequencies," *Biomechanics and Modeling in Mechanobiology* 23, no. 4 (2024): 1369–1376.

30. M. Wiertelwski and V. Hayward, "Mechanical Behavior of the Fingertip in the Range of Frequencies and Displacements Relevant to Touch," *Journal of Biomechanics* 45, no. 11 (2012): 1869–1874.
31. C. D. Shultz, M. A. Peshkin, and J. E. Colgate, "On the Electrical Characterization of Electroadhesive Displays and the Prominent Interfacial Gap Impedance Associated with Sliding Fingertips," In Proceedings of the 2018 IEEE Haptics Symposium (HAPTICS), (IEEE, 2018): 151–157.
32. E. AliAbbasi, M. Muzammil, O. Sirin, P. Lefèvre, Ø. G. Martinsen, and C. Basdogan, "Effect of Finger Moisture on Tactile Perception of Electroadhesion," *IEEE Transactions on Haptics* 17, no. 4 (2024): 841–849.
33. M. J. Adams, S. A. Johnson, P. Lefèvre, et al., "Finger Pad Friction and Its Role in Grip and Touch," *Journal of the Royal Society Interface* 10, no. 80 (2013): 20120467.
34. N. Huloux, L. Willemet, and M. Wiertelwski, "How to Measure the Area of Real Contact of Skin on Glass," *IEEE Transactions on Haptics* 14, no. 2 (2021): 235–241.
35. A. E. Kovalev, K. Dening, B. N. Persson, and S. N. Gorb, "Surface Topography and Contact Mechanics of Dry and Wet Human Skin," *Beilstein Journal of Nanotechnology* 5, no. 1 (2014): 1341–1348.

Supporting Information

Additional supporting information can be found online in the Supporting Information section.